Supporting Information for

Comprehensive Analysis of C–H···π(alkyne) Interactions in Crystal Packing of Diastereomers of 1,2-Di(7′-methoxynaphth-1′-yl)-3,6-di(4″-*n*–propylphenylethynyl)benzene

Minami Nakamura,[a] *Yukiyasu Kashiwagi,*[b] *and Mitsuhiko Morisue** [a]

[a]Faculty of Molecular Chemistry and Engineering, Kyoto Institute of Technology, Matsugasaki, Sakyo-ku, Kyoto 606-8585, Japan, and [b]Osaka Research Institute of Industrial Science and Technology, 1-6-50, Morinomiya, Joto-ku, Osaka 536-8553, Japan

1. Synthesis

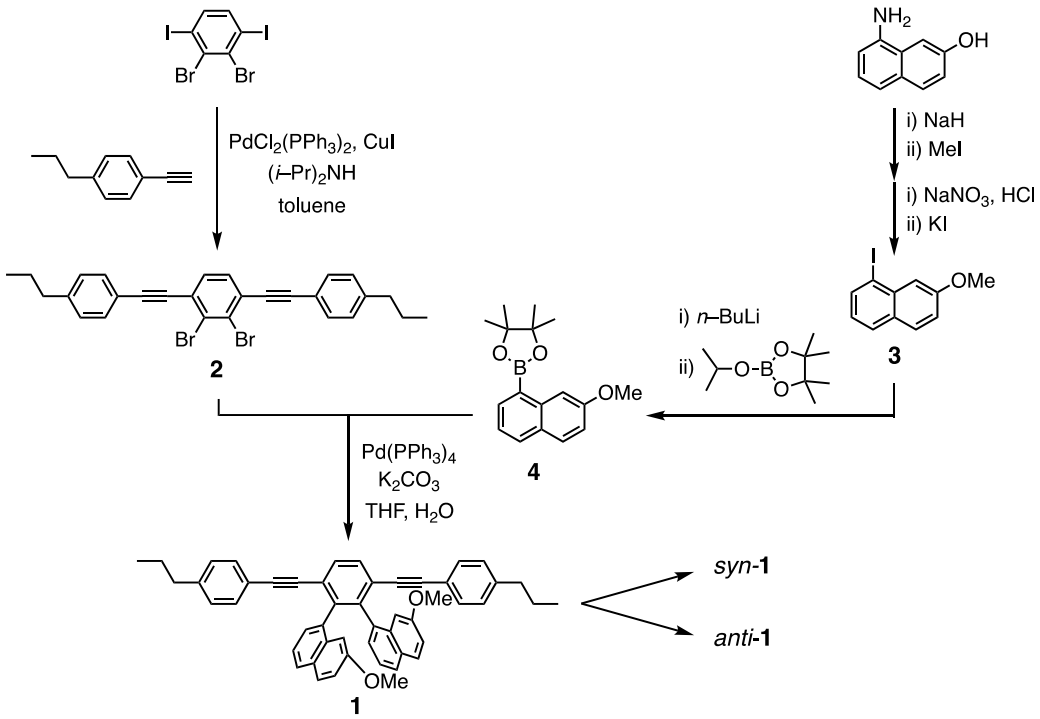

Scheme 1. Synthetic procedures of *syn*- and *anti*-**1**.

1,2-Dibromo-3,6-di(4′-*n*–propylphenylethynyl)benzene (2): In a Schlenk flask, 1,4-diiode-2,3-dibromobenzene (prepared according to the reported method;[S1] 0.30 g, 0.63 mmol) and CuI (4.0 mg, 21 μmol) were dried under vacuum. The mixture was dissolved in toluene (7 mL) and diisopropylamine (0.28 mL) and degassed by successive freeze-pump-thaw cycles before backfilling with Ar. To the solution was added $PdCl_2(PPh_3)_2$ (8.3 mg, 12 μmol) and 4-*n*–propylphenylacetylene (purchased from Tokyo Chemical Industry and used as received; 0.24 mL, 1.5 mmol) under Ar stream. The mixture was gently refluxed at 70 °C for 18 h under the Ar atmosphere. The reaction mixture was successively washed with aqueous NH_3, water, and brine. The organic layer was separated, and the crude material was subjected to silica gel column chromatography with toluene, followed by the additional silica gel column chromatography with *n*–hexane/EtOAc (100/0–50/1, v/v) as the eluent. **2** was isolated as a colorless solid in 74% yield (239 mg, 0.46 mmol). ^{1}H NMR ($CDCl_3$, 500 MHz): δ 7.49 (d, 4H, J = 8.0 Hz), 7.44 (s, 2H), 7.19 (d, 4H, J = 8.0 Hz), 2.61 (t, 4H, J = 7.7 Hz), 1.69–1.61 (m, 4H), 0.95 (t, 6H, J = 7.7 Hz). ^{13}C{^{1}H } NMR ($CDCl_3$, 125 MHz): δ 144.11, 131.70, 130.94, 128.66, 128.56, 126.99, 119.67, 96.26, 88.04, 38.04, 24.34, 13.75.

1-Iodo-7-methoxynaphthalene (3): To a stirring suspension of sodium hydride (0.59 g, 25 mmol) in DMF (40 mL) was added portionwise 7-amino-2-naphthol (3.0 g, 19 mmol) at 0 °C. After stirring for 10 min, methyl iodide (1.2 mL, 19 mmol) was dropwisely added to the mixture at 0 °C followed by additional stirring at room temperature for 16 h. The reaction mixture was diluted with EtOAc and washed with brine. The organic layer was dried over anhydrous magnesium sulfate. After the removal of the solvent, the crude product including 1-amino-6-methoxynaphthalene was obtained as brown syrup. This material was somewhat air-sensitive judging from ^{1}H NMR observation, and was used in the subsequent Sandmeyer reaction step without further purification. The crude product in acetone (200 mL) was diluted with 2 M hydrochloric acid (100 mL) at 0 °C. To the solution was added portionwise $NaNO_2$ (1.2 g, 17 mmol) at 0 °C. The resultant orange diazonium solution was poured into a vigorously stirred solution of potassium iodide (2.8 g, 17 mmol) in water (40 mL). The mixture was allowed to warm up to room temperature with stirring for 17 h. The reaction mixture was neutralized with aqueous $NaHCO_3$. After condensation of the mixture, the residue dissolved in toluene was washed with aqueous $Na_2S_2O_3$ and brine. The organic layer was separated and dried over anhydrous magnesium sulfate. After the removal of the solvent, the crude material was passed through a silica pad with *n*–hexane/toluene (1/1, v/v) as the eluent, followed by the additional purification with silica gel column chromatography using *n*–hexane/toluene (5/1 and then 1/1, v/v) as the eluent.

Recrystallization of the eluted material from dichloromethane/MeOH gave **3** as a white solid in 27% yield (1.43 g, 5.0 mmol) over the two steps. ^{1}H NMR ($CDCl_3$, 500 MHz): δ 8.05–8.03 (m, 1H), 7.76 (d, 1H, J = 8.1 Hz), 7.67 (d, 1H, J = 8.9 Hz), 7.39 (d, 1H, J = 2.5 Hz), 7.16 (dd, 1H, J = 8.9, 2.5 Hz), 7.06–7.03 (m, 1H), 3.89 (s, 3H). ^{13}C{^{1}H} NMR ($CDCl_3$, 125 MHz): δ 159.5, 138.1, 125.9, 130.5, 129.7, 128.9, 124.8, 119.8, 110.8, 98.4, 55.67.

4,4,5,5-Tetramethyl-2-(7′-methoxynaphth-1′-yl)-1,3,2-dioxaborolane (4): A solution of **3** (0.50 g, 1.8 mmol) dissolved in Et_2O (20 mL). To the solution was added dropwise *n*–butyllithium (2.0 M in hexanes, 1.2 mL, 2.4 mmol) at –78 °C. The mixture was stirred at -78 °C for 1 h, followed by the subsequent addition of 2-isopropoxy-4,4,5,5-tetramethyl-1,3,2-dioxaborolane (0.4 mL, 1.9 mmol). The reaction mixture was allowed to warm up to room temperature. After stirring for 20 h, the mixture was poured into aqueous NH_4Cl, the product was extracted with EtOAc, and washed with water and brine. The crude material was purified by silica gel column chromatography with toluene, and then the additional silica gel column chromatography with *n*–hexane/EtOAc (5/1, v/v) as the eluent. **4** was isolated as a pale brown wax in 59% yield (295 mg, 1.04 mmol). ^{1}H NMR ($CDCl_3$, 500 MHz): δ 8.22 (d,1H, J = 2.5 Hz), 8.03 (d, 1H, J = 7.0 Hz), 7.85 (d, 1H, J = 7.9 Hz), 7.72 (d, 1H, J = 8.9 Hz), 7.33 (dd, 1H, J = 7.9, 7.0 Hz), 7.13 (dd, 1H, J = 8.9, 2.5 Hz), 3.94 (s, 3H), 1.41 (s, 12H). ^{13}C{^{1}H} NMR ($CDCl_3$, 125 MHz): δ 158.11, 138.51, 136.28, 131.52, 129.82, 128.84, 122.93, 118.12, 107.23, 83.74, 55.19, 25.16.

1,2-Di(7′-methoxynaphth-1′-yl)-3,6-(4′′-*n*–propylphenylethynyl)benzene (*syn*-1 and *anti*-1): In a two-necked flask, **2** (67 mg, 0.13 mmol), **4** (80 mg, 0.28 mmol) and K_2CO_3 (89 mg, 0.65 mmol) were dried under vacuum before backfilling with Ar. The mixture was dissolved in pre-degassed THF (13 mL) and H_2O (6.5 mL). To the solution was added $Pd(PPh_3)_4$ (27 mg, 24 μmol) under Ar stream. The mixture was gently refluxed at 70 °C for 20 h under the Ar atmosphere. After removal of the organic solvent under reduced pressure, the residue dissolved in $CHCl_3$ was successively washed with water and brine. The crude material was purified by silica gel column chromatography with $CHCl_3$ as the eluent. Subsequently, *anti-1* and then *syn*-**1** were successively eluted from silica gel column chromatography with *n*–hexane/toluene (2/3, v/v). *Syn*-**1** and *anti*-**1** were isolated in 33% yield (29 mg, 43 μmol) and in 63% yield (55 mg, 81 μmol), respectively. ***syn*-1:** ^{1}H NMR (500 MHz, $CDCl_3$): δ 7.73 (s, 2H), 7.55 (d, 2H, J = 8.9 Hz), 7.52 (d, 2H, J = 8.2 Hz), 7.34–7.32 (m, 2H), 7.15 (dd, J = 8.2, 7.1 Hz, 2H), 7.00 (d, 2H, J = 2.5 Hz), 6.92 (dd, 2H, J = 8.9, 2.5 Hz), 6.88 (d, 4H, J = 8.2 Hz), 6.56 (d, 4H, J

= 8.2 Hz), 3.66 (s, 6H), 2.44 (t, 4H, J = 7.6 Hz), 1.54–1.49 (m, 4H), 0.85 (t, 6H, J = 7.5 Hz). $^{13}C\{^1H\}$ NMR (125 MHz, $CDCl_3$): δ 156.95, 143.44, 142.91, 135.62, 132.88, 131.12, 130.74, 129.67, 129.35, 128.75, 128.14, 127.09, 124.90, 122.23, 120.12, 117.14, 106.21, 94.92, 88.76, 55.18, 37.87, 24.22, 13.70. λ_{max}/nm (ε/mM^{-1} cm^{-1}) at 298 K in $CHCl_3$: 334 (72.2), 356.5 (61.9). Φ_F = 0.322 (λ_{em} = 367.5, 400.5 nm). ***anti*-1:** ^1H NMR (500 MHz, $CDCl_3$): δ 7.72 (s, 2H), 7.68 (d, 2H, J = 8.9 Hz), 7.51 (d, 2H, J = 8.1 Hz), 7.11 (dd, 2H, J = 8.9, 2.5 Hz), 7.05 (d, 2H, J = 2.5 Hz), 6.96 (d, 2H, J = 7.1 Hz), 6.88 (d, 4H, J = 8.1 Hz), 6.86 (d, 2H, J = 7.1 Hz), 6.52 (d, 4H, J = 8.1 Hz), 3.81 (s, 6H), 2.44 (t, 4H, J = 7.6 Hz), 1.53–1.49 (m, 4H), 0.84 (t, 6H, J = 7.4 Hz). $^{13}C\{^1H\}$ NMR (125 MHz, $CDCl_3$): δ 157.58, 143.54, 142.95, 136.38, 133.54, 131.08, 130.62, 129.46, 128.65, 128.14, 127.11, 126.58, 124.78, 122.64, 120.01, 117.96, 104.93, 94.96, 88.54, 55.36, 37.87, 24.21, 13.69. λ_{max}/nm (ε/mM^{-1} cm^{-1}) at 298 K in $CHCl_3$: 334 (83.2), 356 (71.5). Φ_F = 0.334 (λ_{em} = 366, 396 nm).

[S1] V. Diemer, F. R. Leroux, F. Colobert, *Eur. J. Org. Chem.* 2011, 327–340.

2. Electronic Properties

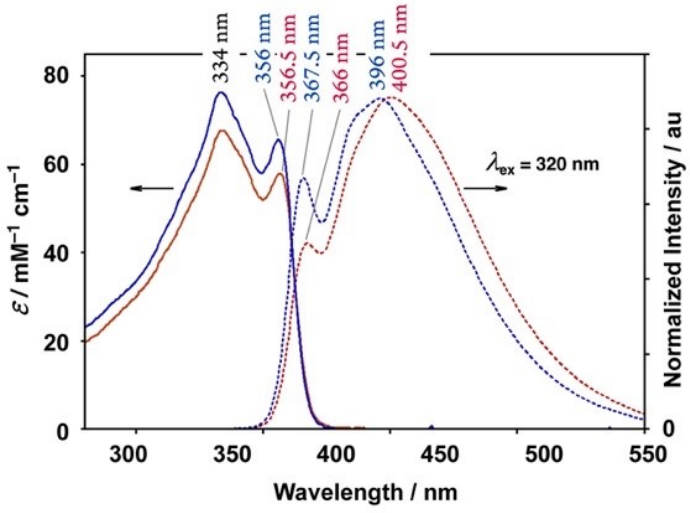

Fig S1. Electronic absorption (solid line) and fluorescence spectra (dotted line) of *syn*-**1** (red) and *anti*-**1** (blue) in chloroform. Fluorescence spectra were observed by excitation at 320 nm. The absolute fluorescence quantum yield (Φ_F) is 0.322 for *syn*-**1** and 0.334 for *anti*-**1**.

3. Details of Crystal Structures

Table S1. Properties of possible C–H···π interactions.

Short Contact		Atoms	Distance [a] / Å	Bond descriptors (van der Waals crust) [c]		Topological descriptors at bond critical points (QTAIM) [b]		
				i_{CH} / Å	p_{CH} / %	ρ_{BCP} / e au^{-3}	$\nabla^2\rho_{BCP}$ / e au^{-5}	H_{BCP} / au
***syn*-1**	C–H···π(alkyne)	C8–H8···C43^{i}	2.728(7)	0.24	12.74	nd	nd	nd
		C49–H49···C34^{ii}	2.778(7)	0.19	10.11	0.0050	0.0166	0.0009
		C19–H19···C42^{i}	2.755(6)	0.22	11.32	nd	nd	nd
		C46–H46···C34^{i}	2.893(7)	0.08	4.05	0.0044	0.0150	0.0009
		C24–H24···C34^{iii} (C24–H24···*Cg*2^{iii})	3.174(7) (3.066)	–0.20	–10.74	0.0042	0.0131	0.0008
	Intramolecular C–H···π(alkyne) contact	C30–H30···C11	3.144(7)	–0.17	–9.16	0.002498	0.007458	0.000431
		C45–H45···C20	3.428(7)	–0.46	–24.11	0.001541	0.04493	0.000285
	C–H···π(arene)	C32–H32···C24^{iii} (C32–H32···*Cg*1^{iii})	2.608(7) (2.858)	0.36	19.05	0.0072	0.0224	0.0011
		C19–H19···C39	2.711(7)	0.26	13.63	0.0056	0.0190	0.0010
		C8–H8···C44^{i}	2.753(7)	0.22	11.42	0.0058	0.0206	0.0012
		C20–H20···C40^{i}	2.915(6)	0.06	2.89	0.004271	0.013424	0.000779
		C41–H41···C16^{ii}	2.938(6)	0.03	1.68	0.003901	0.013603	0.000848
		C33–H33···C13^{iii}	3.044(7)	–0.07	–3.89	0.003338	0.009800	0.000545
***anti*-1**	C–H···π(alkyne)	C45–H45···C31^{i}	2.65(1)	0.32	16.95	nd	nd	nd
		C44–H44···C30^{i}	3.22(1)	–0.26	–13.42	0.0024	0.0079	0.0005
		C12^{i}–H12^{i}···C42	3.56(1)	–0.59	–31.16	0.0017	0.0057	0.0003
	Intramolecular C–H···π(arene) contact	C48^{ii} –H48^{ii} ···C23^{ii}	3.43(1)	–0.46	–24.26	0.001543	0.005049	0.000321
		C33–H33···C9	2.73(1)	0.24	12.47	0.005483	0.018315	0.000889
		C33^{ii} –H33^{ii} ···C9^{ii}	2.73(1)	0.24	12.47	0.005480	0.018291	0.000888
		C48–H48···C23	3.43(1)	–0.46	–24.26	0.001540	0.005060	0.000322
	C–H···π(arene)	C21^{ii}–H21^{ii}···C25	2.59(1)	0.38	19.95	0.0068	0.0221	0.0012
		C45–H45···C32^{i}	2.57(1)	0.40	20.95	0.0068	0.0228	0.0012
		C17–H17···C26^{i}	2.68(1)	0.29	15.26	nd	nd	nd
		C16–H16···C25^{i}	2.71(1)	0.26	13.42	0.0054	0.0206	0.0013
		C47–H47···C10^{ii}	2.80(1)	0.17	9.16	0.0057	0.0183	0.0010
		C44–H44···C12^{i}	2.85(1)	0.12	6.05	0.00397	0.1171	0.000655

4. *a*) The interatomic distance (d_{CH}) from the proton to the proximal carbon or centroid along the C–H···π contacts with the Hirshfeld-atom refinement. *b*) Bond descriptors for the C···H contact; penetration index (i_{CH}) and dimensionless penetration index (p_{CH}) (see Fig 7). *c*) Topological descriptors at the bond critical points; electron density (ρ_{BCP}), its Laplacian ($\nabla^2\rho_{BCP}$), and the energy density (H_{BCP}). See Table 1 for the C–H···π interactions with short contact. *Cg*1 is the centroid of the C15–C17/C22–C24 ring and *Cg*2 is the centroid of the C34≡C35 bond.

Table S2. Crystal detail of *syn*-1,2-di(7′-methoxynaphth-1′-yl)-3,6-di(4″-*n*-propylphenylethynyl)benzene (*syn*-**1**).

CCDC code		2313036
Chemical Formula		$C_{50}H_{42}O_2$
M_r		674.83
Crystal system, space group		Triclinic, $P\bar{1}$
Temperature / K		100
a, *b*, *c* / Å		9.5381 (1), 11.0760 (1), 18.5558 (2)
α, β, γ / °		97.365 (1), 102.275 (1), 93.924 (1)
V (Å^3)		1890.41 (3)
Z		2
Radiation type		Cu *K*α
μ / mm^{-1}		0.54
Crystal size / mm		0.42 × 0.18 × 0.05
Data collection	Diffractometer	XtaLAB Synergy, Dualflex, HyPix
	Absorption correction	Multi-scan *CrysAlis PRO* 1.171.42.63a (Rigaku Oxford Diffraction, 2022) Empirical absorption correction using spherical harmonics, implemented in SCALE3 ABSPACK scaling algorithm.
	T_{min}, T_{max}	0.426, 1.000
	No. of measured, independent and observed [I > 2σ(I)] reflections	58698, 7493, 6479
	R_{int}	0.047
	(sing θ/λ)max / Å^{-1}	0.632
Refinement	$R[F^2 > 2\sigma(F^2)]$, $wR(F^2)$, S	0.038, 0.103, 1.08
	No. of reflections	7493
	No. of parameters	473
	H-atom treatment	H-atom parameters constrained
	$\Delta\rho_{max}$, $\Delta\rho_{min}$ / e Å^{-3}	0.18, –0.24

Computer programs: *CrysAlis PRO* 1.171.42.63a (Rigaku OD, 2022), SHELXT (Sheldrick, 2015), *SHELXL* 2018/3 (Sheldrick, 2015), *OLEX2* 1.5 (Dolomanov *et al.*, 2009).

Table S3. Crystal detail of *anti*-1,2-di(7′-methoxynaphth-1′-yl)-3,6-di(4″-*n*-propylphenylethynyl)benzene (*anti*-**1**).

CCDC code		2325068
Chemical Formula		$C_{50}H_{42}O_2$
M_r		674.83
Crystal system, space group		Orthorhombic, $P2_12_12_1$
Temperature / K		100
a, *b*, *c* / Å		13.4062 (1), 13.4800 (1), 20.5669 (2)
V (Å^3)		3716.76 (5)
Z		4
Radiation type		Cu *K*α
μ / mm^{-1}		0.55
Crystal size / mm		0.18 × 0.16 × 0.06
Data collection	Diffractometer	XtaLAB Synergy, Dualflex, HyPix
	Absorption correction	Multi-scan *CrysAlis PRO* 1.171.42.90a (Rigaku Oxford Diffraction, 2023) Empirical absorption correction using spherical harmonics, implemented in SCALE3 ABSPACK scaling algorithm.
Refinement	T_{min}, T_{max}	0.922, 1.000
	No. of measured, independent and observed [I > 2σ(I)] reflections	23457, 7386, 7014
	R_{int}	0.036
	(sing θ/λ)max / Å^{-1}	0.633
	$R[F^2 > 2\sigma(F^2)]$, $wR(F^2)$, S	0.030, 0.075, 1.06
	No. of reflections	7386
	No. of parameters	473
	H-atom treatment	H-atom parameters constrained
	$\Delta\rho_{max}$, $\Delta\rho_{min}$ / e Å^{-3}	0.12, –0.18
	Absolute structure	Flack x determined using 2920 quotients [(I+)–(I–)]/[(I+)+(I–)] (Persons, Flack and Wagner, Acta Cryst. B69 (2013) 249–259).
	Absolute structure parameter	–0.18 (10)

Computer programs: *CrysAlis PRO* 1.171.42.90a (Rigaku OD, 2023), SHELXT 2018/2 (Sheldrick, 2018), *SHELXL* 2018/3 (Sheldrick, 2015), *OLEX2* 1.5-ac-5-024 (Dolomanov *et al.*, 2009).

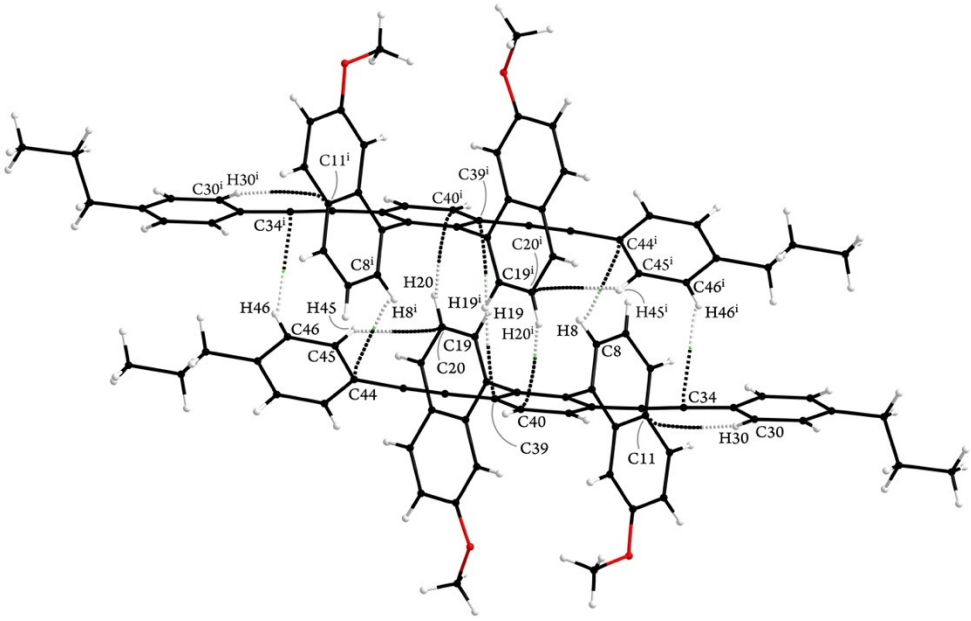

Fig S2. All bond paths along the C–H···π geometries in the crystal packing of *syn*-**1** (Fig 3A). The contour map of electron density is shown in Fig 8B and 8D. Bond paths along non-covalent bonds other than the C–H···π geometries are omitted for visual clarity.

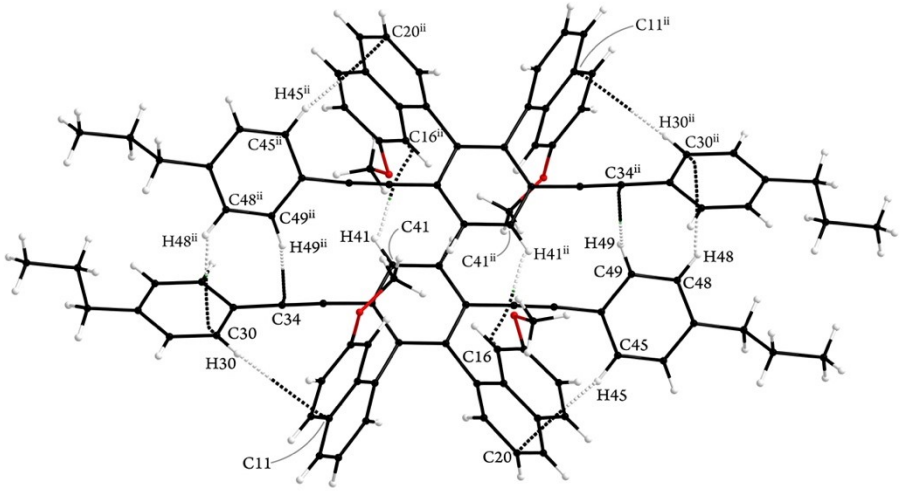

Fig S3. All bond paths along the C–H···π geometries in the crystal packing of *syn*-**1** (Fig 3B). The contour map of electron density is shown in Fig 8A. Bond paths along non-covalent bonds other than the C–H···π geometries are omitted for visual clarity.

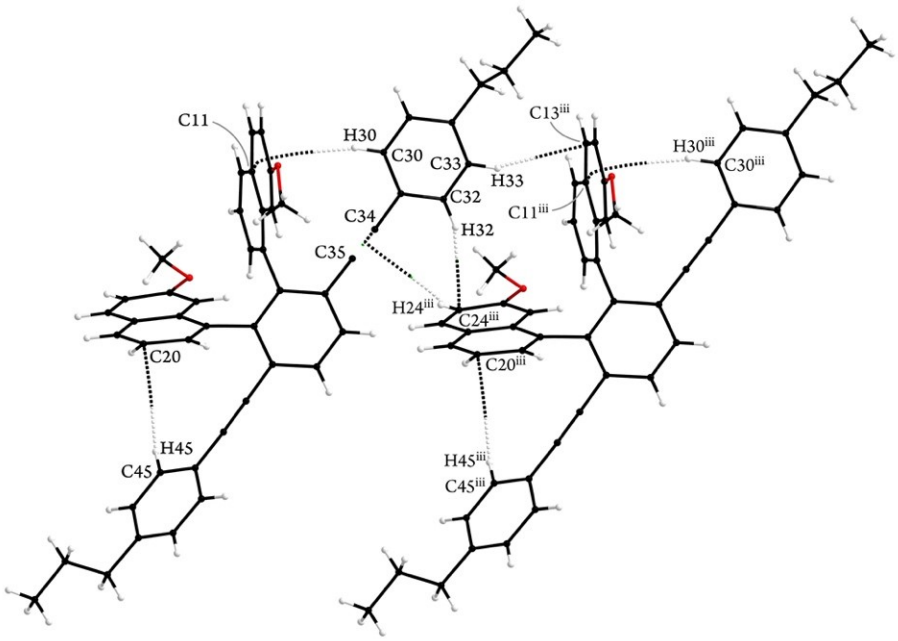

Fig S4. All bond paths along the C–H···π geometries in the crystal packing of *syn*-**1** (Fig 3C). The contour map of electron density is shown in Fig 8C and 8E. Bond paths along non-covalent bonds other than the C–H···π geometries are omitted for visual clarity.

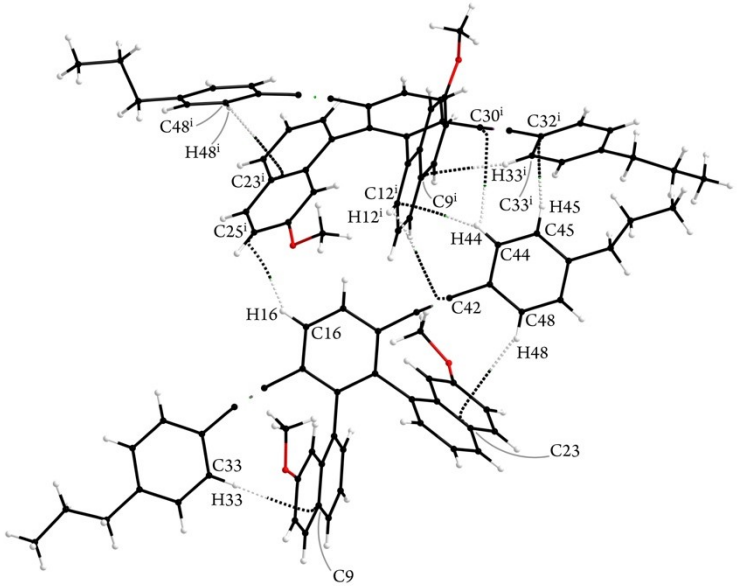

Fig S5. All bond paths along the C–H···π geometries in the crystal packing of *anti*-**1** (Fig 5A). The contour map of electron density is shown in Fig 9A and 9B. Bond paths along non-covalent bonds other than the C–H···π geometries are omitted for visual clarity.

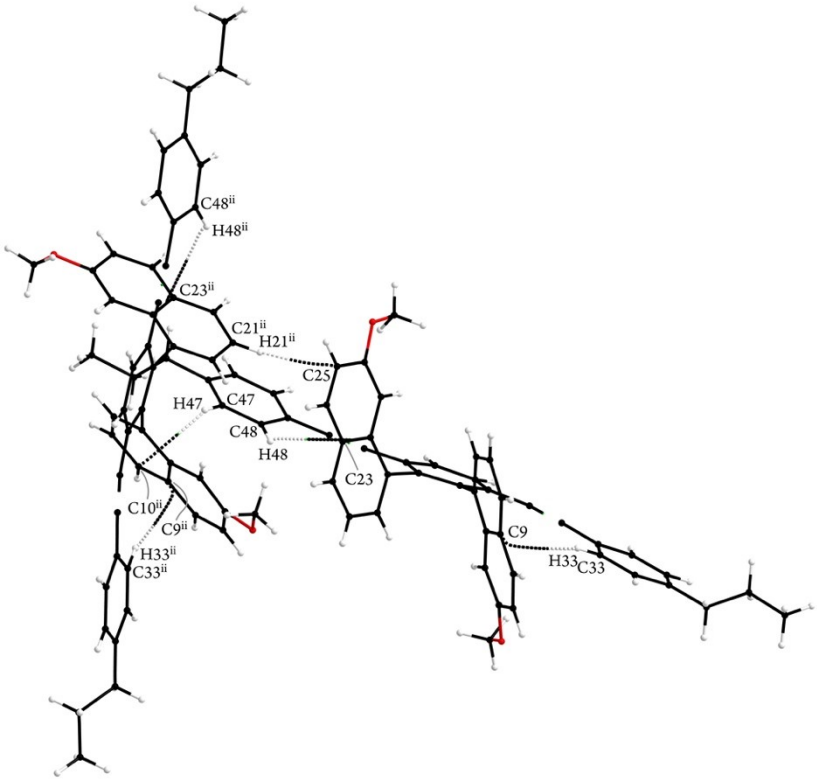

Fig S6. All bond paths along the C–H···π geometries in the crystal packing of *anti*-**1** (Fig 5B). The contour map of electron density is shown in Fig 9C and 9D. Bond paths along non-covalent bonds other than the C–H···π geometries are omitted for visual clarity.

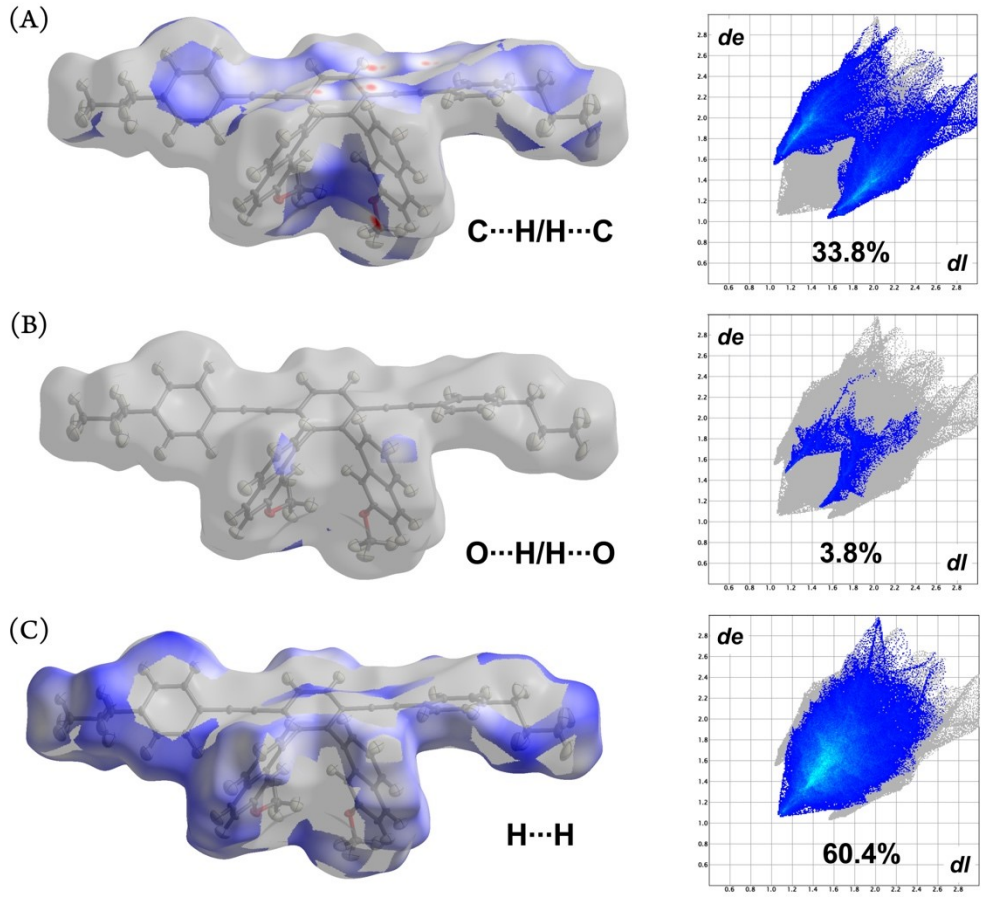

Fig S7. Hirshfeld surfaces of *syn*-**1** mapped for d_{norm} and two-dimensional fingerprint plots for C···H/H···C contacts (A), O···H/H···O contacts (B), and H···H contacts (C).

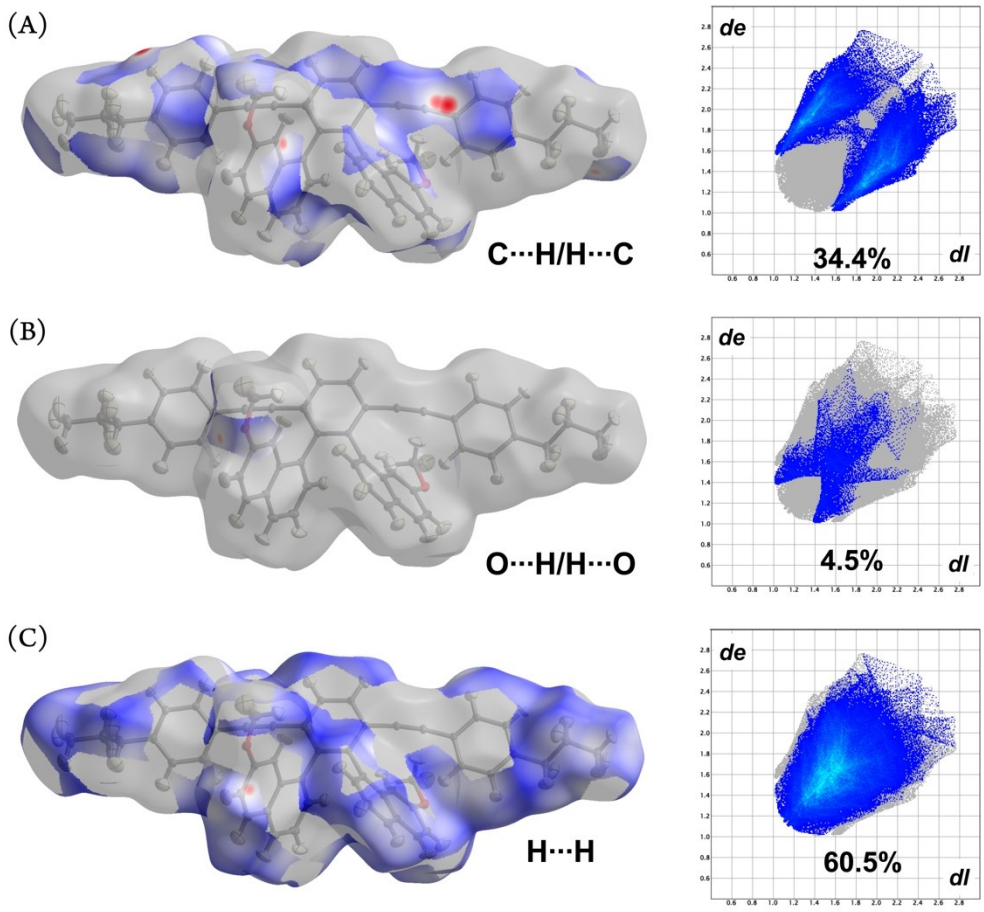

Fig S8. Hirshfeld surfaces of *anti*-**1** mapped for d_{norm} and two-dimensional fingerprint plots for C···H/H···C contacts (A), O···H/H···O contacts (B), and H···H contacts (C).

5. Spectroscopic data of new compounds.

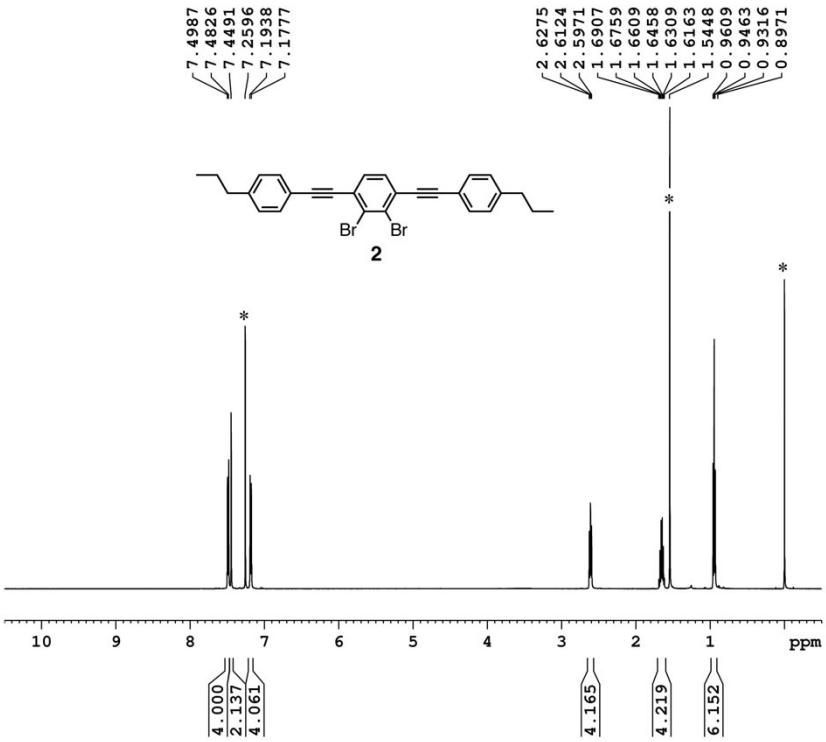

Fig S9. ^{1}H NMR spectrum (500 MHz) of **2** in $CDCl_3$. The asterisk indicates residual solvent, water, and TMS.

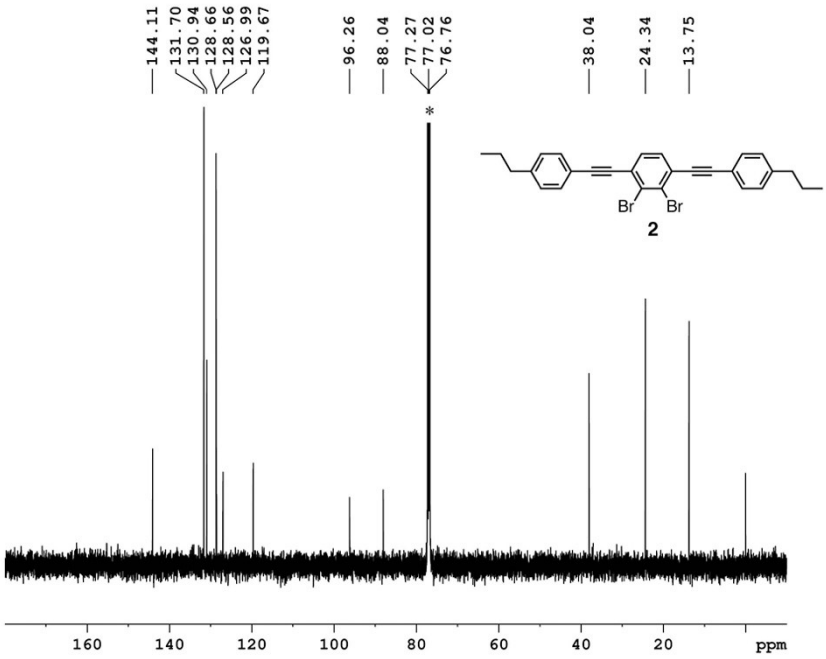

Fig S10. $^{13}C\{^{1}H\}$ NMR spectrum (125 MHz) of **2** in $CDCl_3$. The asterisk indicates solvent.

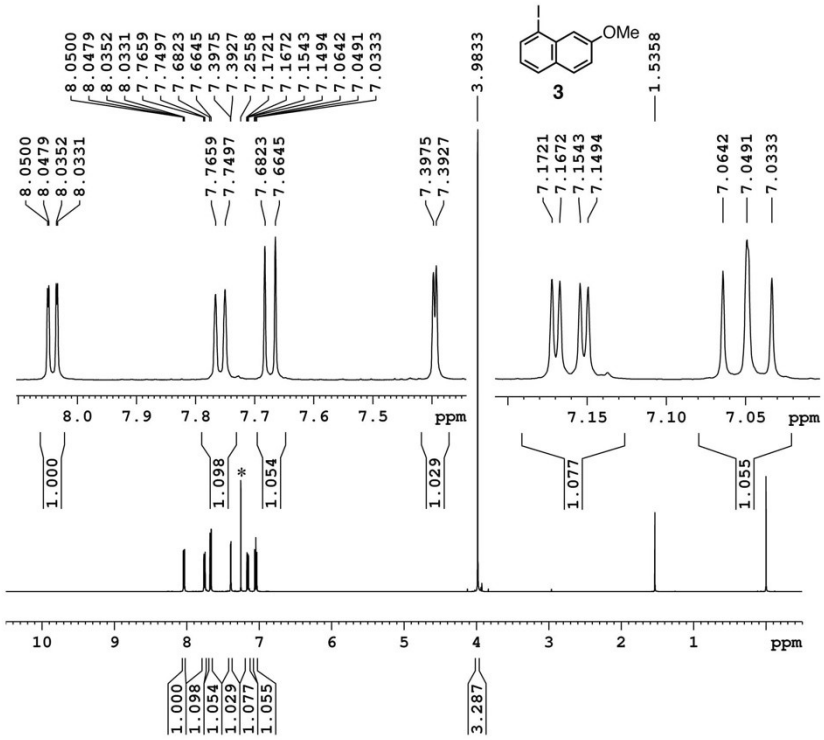

Fig S11. ^{1}H NMR spectrum (500 MHz) of **3** in $CDCl_3$. The asterisk indicates residual solvent.

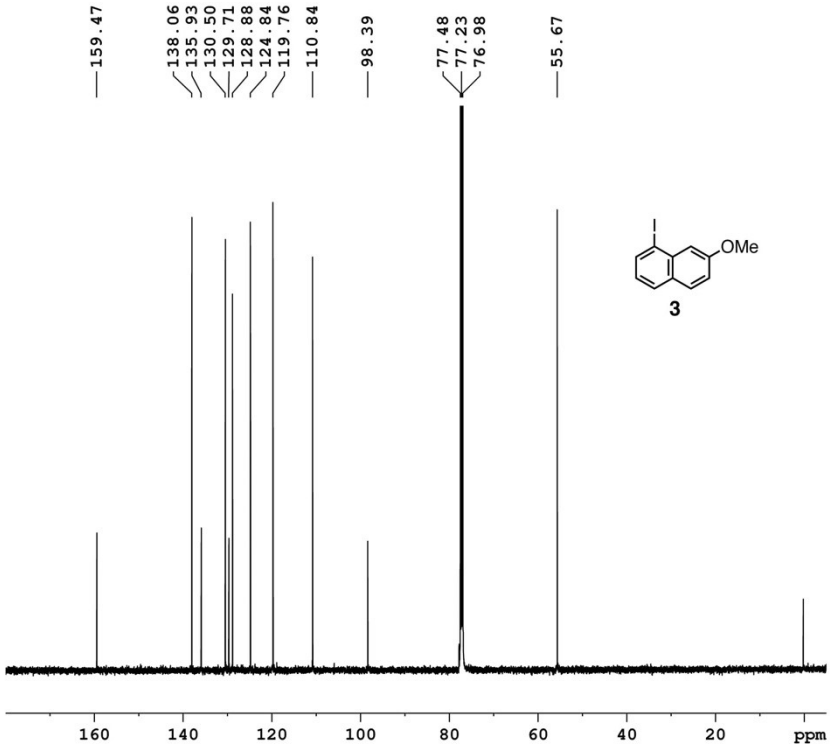

Fig S12. $^{13}C\{^{1}H\}$ NMR spectrum (125 MHz) of **3** in $CDCl_3$. The asterisk indicates solvent.

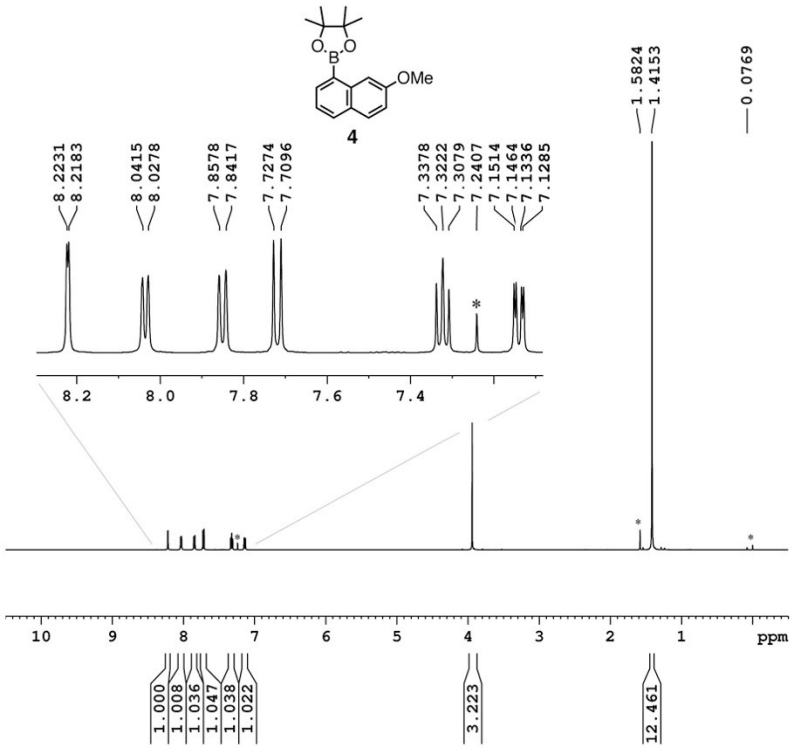

Fig S13. ^{1}H NMR spectrum (500 MHz) of **4** in $CDCl_3$. The asterisk indicates residual solvent, water, and TMS.

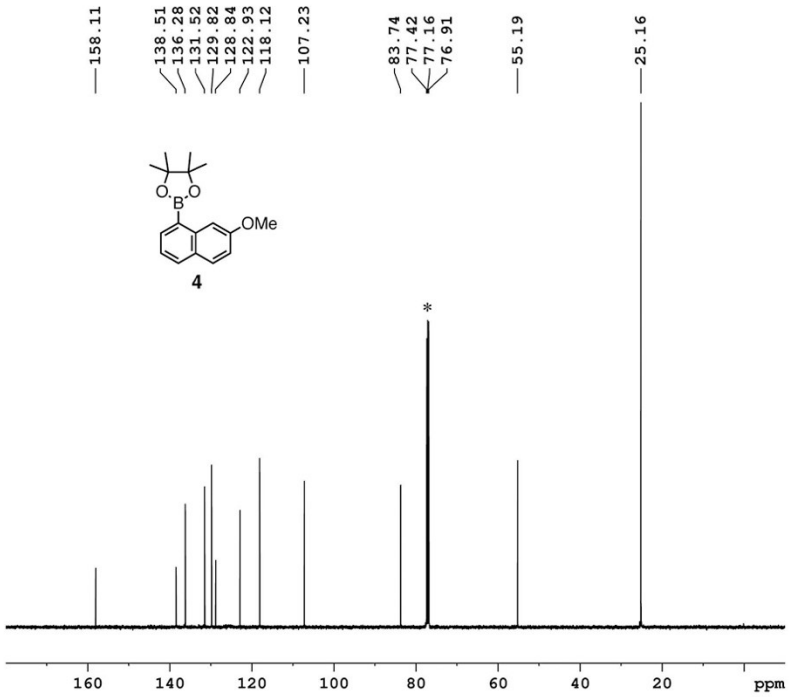

Fig S14. $^{13}C\{^{1}H\}$ NMR spectrum (125 MHz) of **4** in $CDCl_3$. The asterisk indicates solvent.

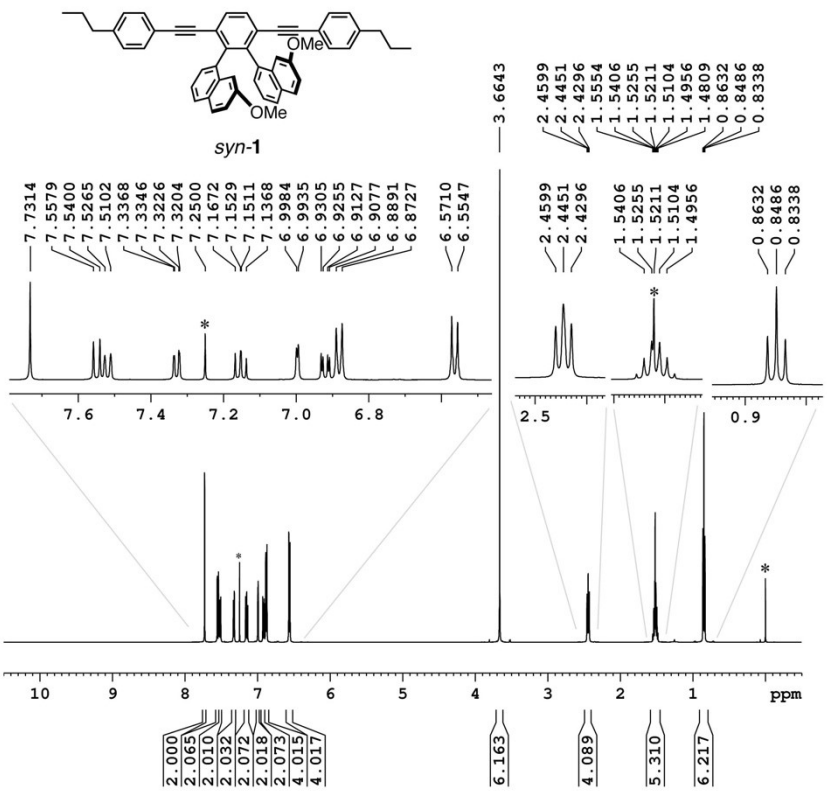

Fig S15. ^{1}H NMR spectrum (500 MHz) of *syn*-**1** in $CDCl_3$. The asterisk indicates residual solvent and TMS.

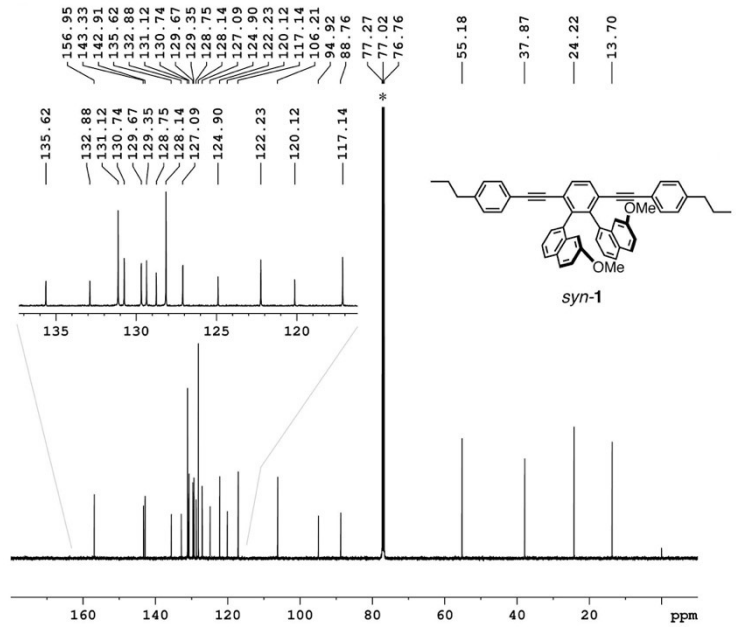

Fig S16. $^{13}C\{^{1}H\}$ NMR spectrum (125 MHz) of *syn*-**1** in $CDCl_3$. The asterisk indicates solvent.

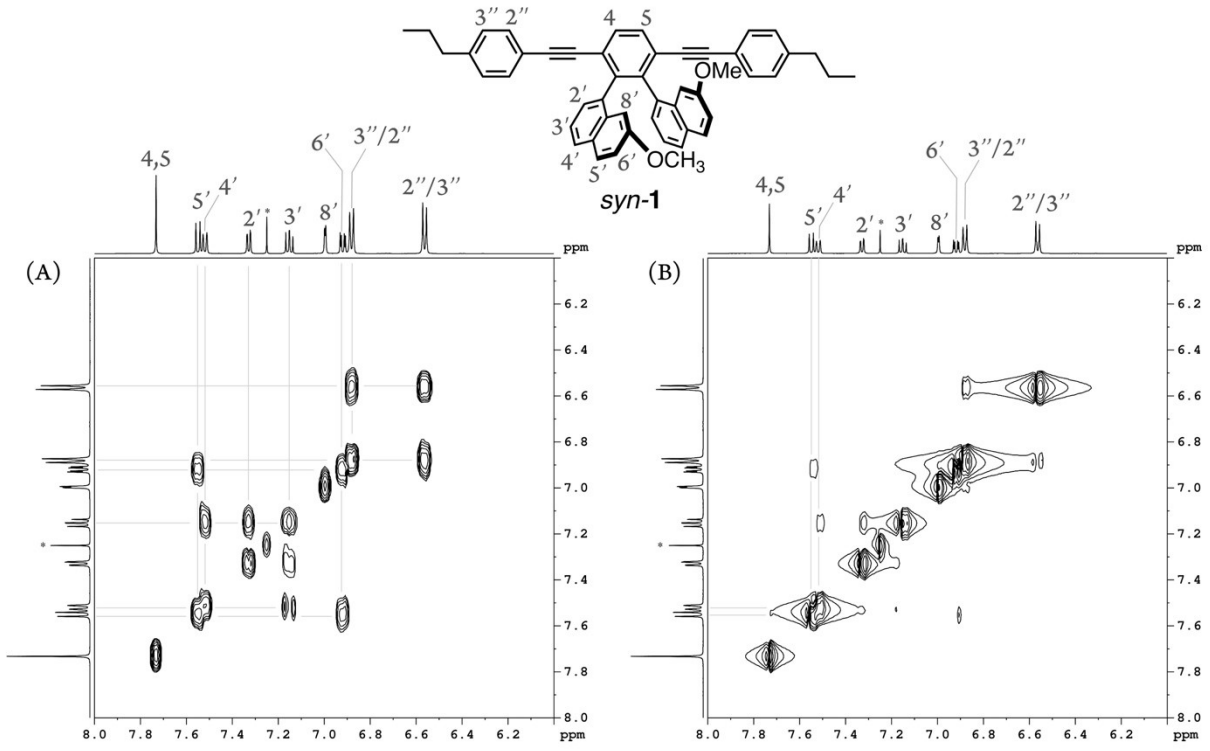

Fig S17. ^{1}H–^{1}H COSY (A) and NOESY spectra (B) of *syn*-**1** in $CDCl_3$. The asterisk indicates residual solvent.

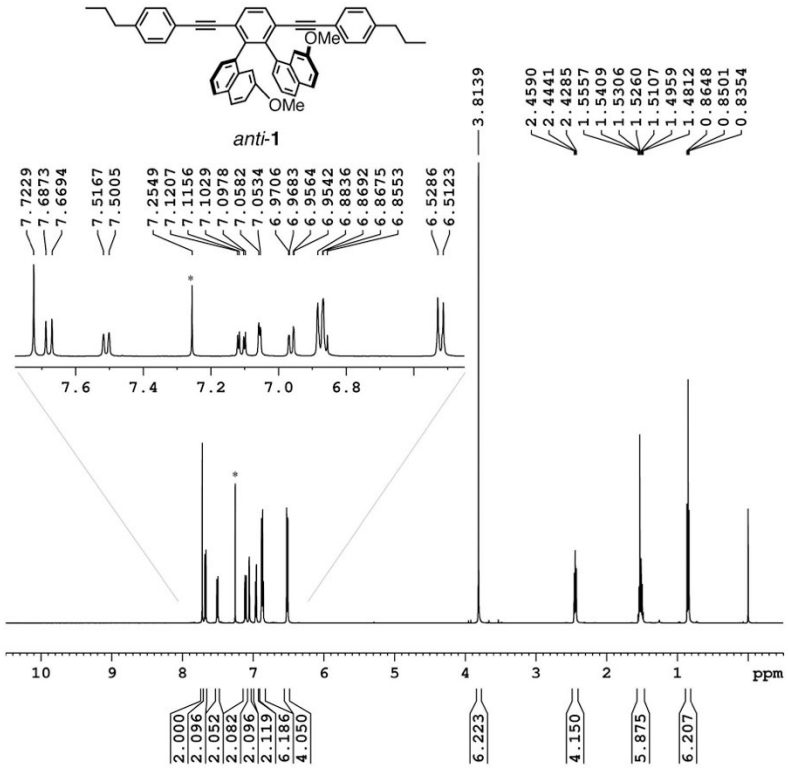

Fig S18. ^{1}H NMR spectrum (500 MHz) of *anti*-**1** in $CDCl_3$. The asterisk indicates residual solvent.

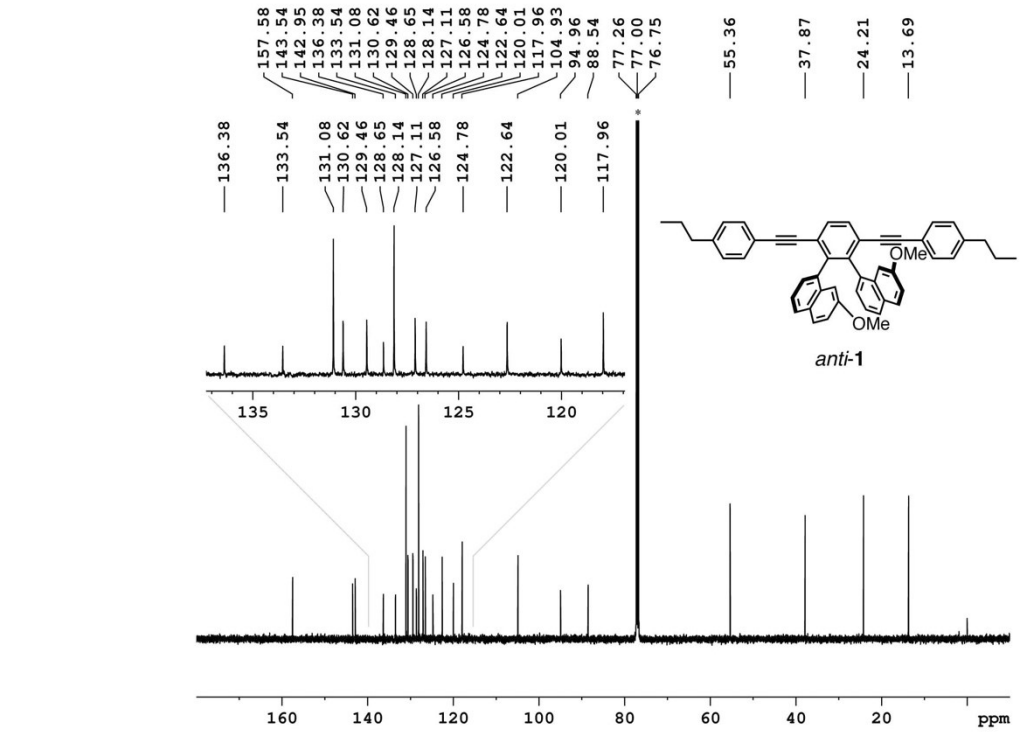

Fig S19. $^{13}C\{^{1}H\}$ NMR spectrum (125 MHz) of *anti*-**1** in $CDCl_3$. The asterisk indicates solvent.

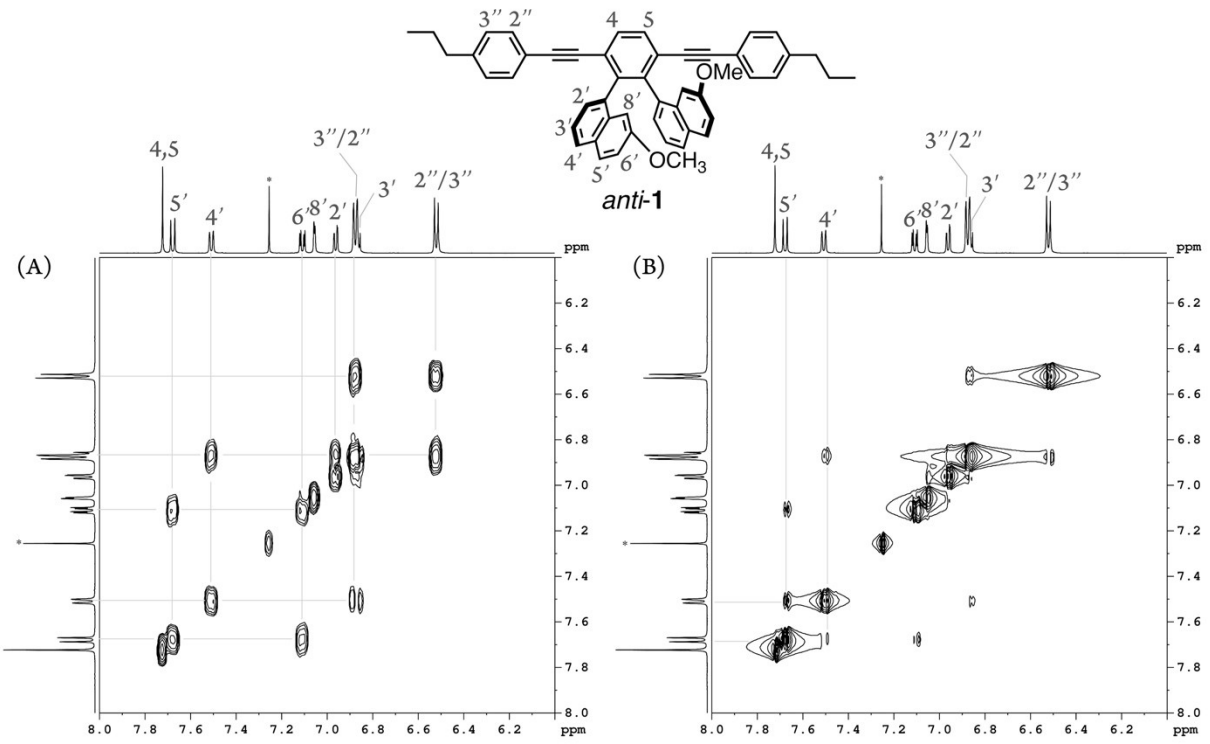

Fig S20. $^{1}H–^{1}H$ COSY (A) and NOESY spectra (B) of *anti*-**1** in $CDCl_3$. The asterisk indicates residual solvent.